

Investigating the reliability of ComBat for harmonizing diffusion MR images acquired at a single site with multiple echo times

Yukai Zou^{1,2}, Yin Jin³, Joseph V. Rispoli^{4,5}

¹ Department of Clinical Neurosciences, University of Southampton, U.K., ² Medical Physics Department, University Hospital Southampton NHS Foundation Trust, U.K.,
³ Department of Biological Sciences, Purdue University, U.S.A., ⁴ Weldon School of Biomedical Engineering, Purdue University, U.S.A., ⁵ School of Electrical and Computer Engineering, Purdue University, U.S.A.

INTRODUCTION

- Precision of diffusion MRI measures is prone to different scanners, acquisition parameters, and other confounding factors such as vendor, bandwidth, head coils, and signal-to-noise ratio. Notably, a strong TE dependence of echo time (TE) was observed for DTI metrics. To date, many harmonization techniques for diffusion MRI have been proposed to perform data pooling from multiple sites and scanners.
- Combined association test (ComBat) has gained popularity for harmonizing MRI data by removing variability introduced by sites and scanners in parametric maps while preserving biological variability.
- **This work aims to investigate whether ComBat can harmonize diffusion MRI data acquired at a single site with multiple TE values.**

METHODS

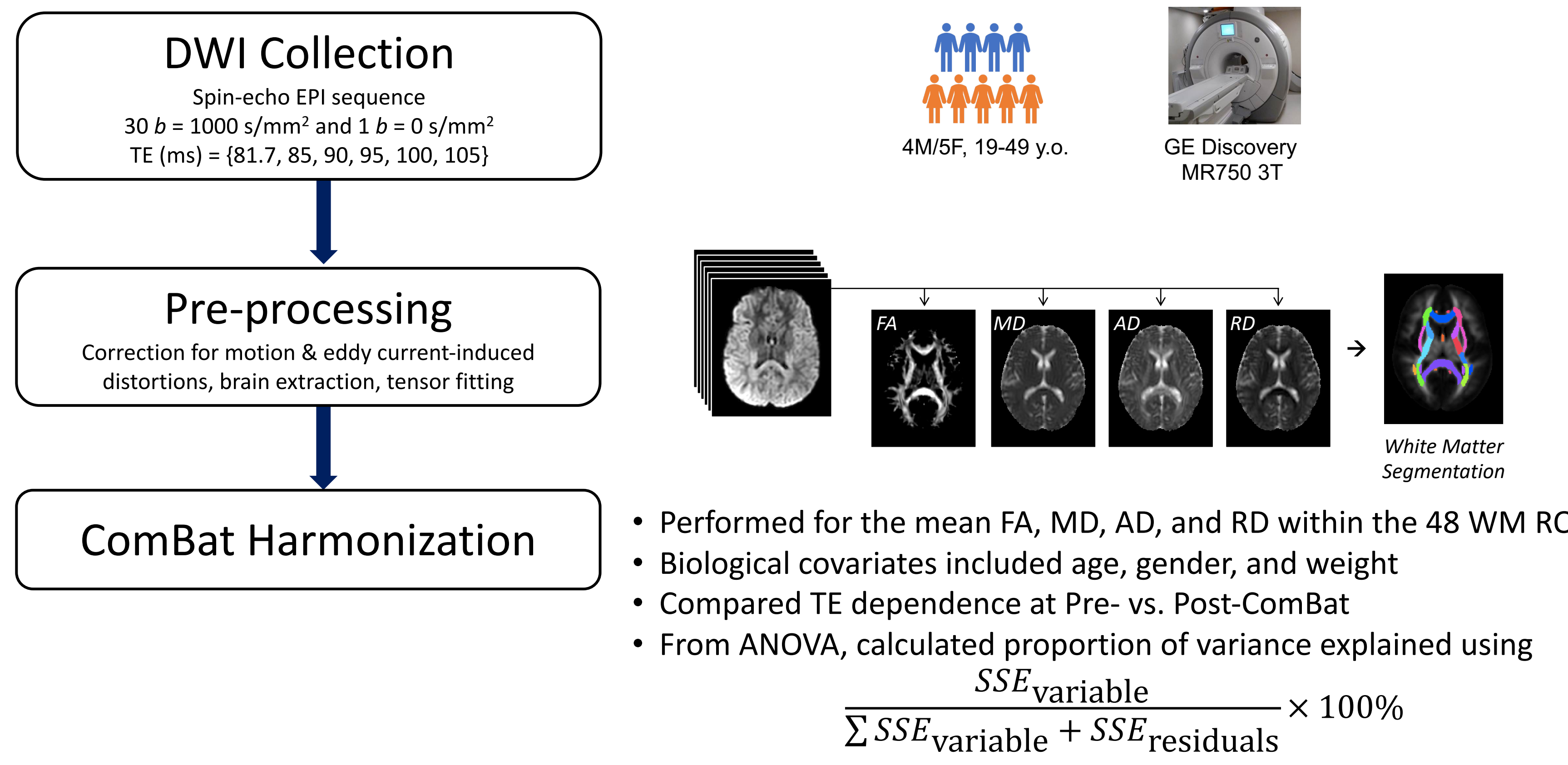


Fig 1: Workflow of collecting and harmonizing single-site multi-TE DWI data.

RESULTS & DISCUSSION

- After ComBat, most of the TE dependence was corrected (Table 1), the biological variabilities were preserved, and the proportion of variance explained by TE was reduced (Fig 2). However, the TE dependence persisted for AD within the right cerebral peduncle (Fig 3A), and for RD within the right superior corona radiata (Fig 3B).
- The removal of TE dependence by ComBat was not always consistent across the ROIs. Because ComBat takes parametric maps as inputs, harmonization may be prone to cases where assumptions on parametric prior distributions are violated.

Table 1: TE dependence before and after ComBat harmonization

	White Matter Tracts	β_{TE}	Pre-ComBat		Post-ComBat	
			p_{TE}	β_{TE}	p_{TE}	β_{TE}
FA	Splenium of corpus callosum	3.39×10^{-4}	0.017	1.64×10^{-4}	0.211	
	Right posterior limb of internal capsule	4.17×10^{-4}	0.012	2.10×10^{-4}	0.169	
	Right medial lemniscus	5.29×10^{-4}	0.012	2.08×10^{-4}	0.243	
	Right corticospinal tract	5.22×10^{-4}	0.034	2.14×10^{-4}	0.343	
	Left superior corona radiata	4.73×10^{-4}	0.025	2.22×10^{-4}	0.260	
MD	Left medial lemniscus	4.76×10^{-4}	0.021	1.90×10^{-4}	0.303	
	Right cerebral peduncle	6.42×10^{-7}	0.022	3.11×10^{-7}	0.221	
	Right cerebral peduncle	1.49×10^{-6}	<0.001	7.81×10^{-7}		
	Left posterior limb of internal capsule	9.41×10^{-7}	0.003	4.33×10^{-7}		
	Left external capsule	8.63×10^{-7}	0.031	3.08×10^{-7}		
AD	Left corticospinal tract	1.63×10^{-6}	0.027	6.32×10^{-7}		
	Left cerebral peduncle	1.48×10^{-6}	0.001	7.04×10^{-7}		
	Right superior corona radiata	-3.91×10^{-7}	0.022	-3.10×10^{-7}		
	Right posterior limb of internal capsule	-3.21×10^{-7}	0.023	-2.48×10^{-7}		
	Left external capsule	5.02×10^{-7}	0.032	2.51×10^{-7}		
RD	Left external capsule	0.048	0.081	0.056		
	Right superior corona radiata	-3.91×10^{-7}	0.022	-3.10×10^{-7}		
	Right posterior limb of internal capsule	-3.21×10^{-7}	0.023	-2.48×10^{-7}		
	Left external capsule	5.02×10^{-7}	0.032	2.51×10^{-7}		
	Left external capsule	0.048	0.081	0.056		

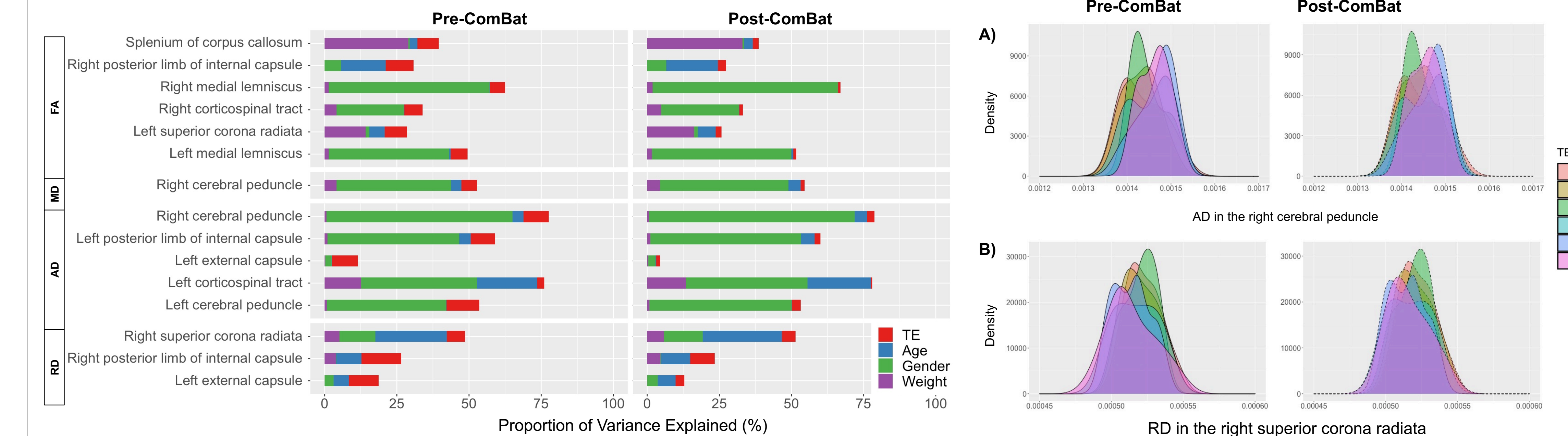


Fig 2: Bar plots illustrating proportion of variance explained by each variable before and after ComBat harmonization.

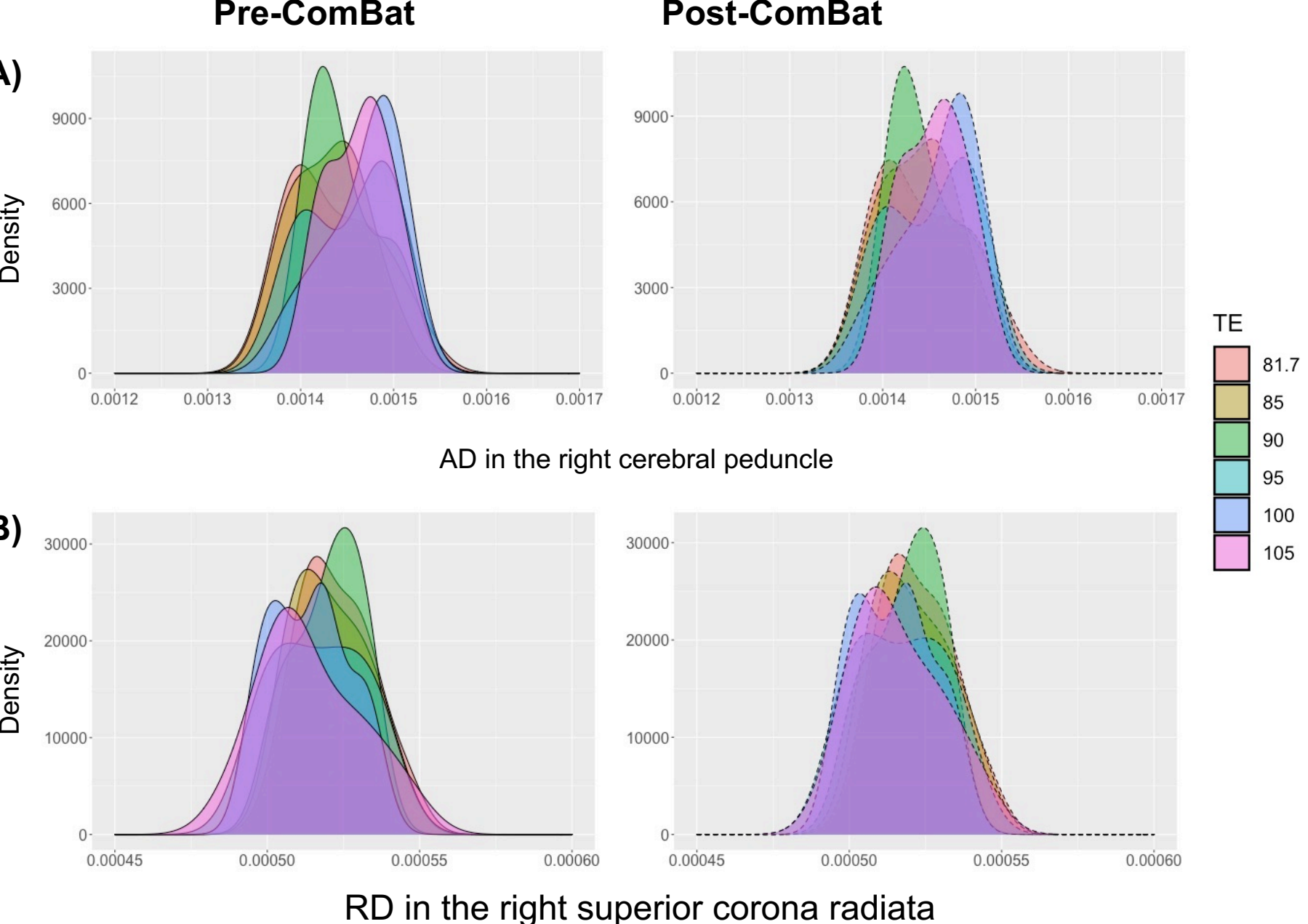


Fig 3: Density plots of A) AD in the right cerebral peduncle and B) RD in the right superior corona radiata, where TE dependence remained after ComBat harmonization.

CONCLUSION

Implement ComBat with caution, even if DWI data are collected from a single site.

REFERENCES: [1] Pinto, M. S. et al., *Front. Neurosci.* 14, 396 (2020). [2] Johnson, W. E., et al., *Biostatistics* 8, 118–127 (2007). [3] Fortin, J.-P. et al., *Neuroimage* 161, 149–170 (2017). [4] Fortin, J. P. et al., *Neuroimage* 167, 104–120 (2018). [5] Nielson, D. M. et al., *bioRxiv* 309260 (2018). [6] Kivrak, A. S. et al., *Diagnostic Interv. Radiol.* 19, 433–437 (2013). [7] Qin, W. et al., *Magn. Reson. Med.* 61, 755–760 (2009). [8] Mirzaalian, H. et al., *Med. Image Comput. Comput. Interv.* 9349, 12–19 (2015). [9] Veraart, J., et al., *Neuroimage* 182, 360–369 (2018). [10] Timmermans, C., et al., *J. Magn. Reson. Imaging* 49, 955–965 (2019). [11] Pomponio, R. et al., *Neuroimage* 208, 116450 (2020). [12] Cetin Karayumak, S. et al., *Neuroimage* 184, 180–200 (2019).

FUNDING: Indiana Clinical and Translational Sciences Institute (EPAR940), and NIH UL1TR002529.